ELSEVIER

www.elsevier.nl/locate/ica

Inorganica Chimica Acta 318 (2001) 103–116

Inorganica Chimica Acta

Heteroleptic 5,5′-disubstituted-2,2′-bipyridine complexes of ruthenium(II): spectral, electrochemical, and structural investigations

Xiao-Juan Yang [a], Christoph Janiak [a,*], Jürgen Heinze [b], Friedrich Drepper [c], Peter Mayer [d], Holger Piotrowski [d], Peter Klüfers [d]

[a] *Institut für Anorganische und Analytische Chemie, Universität Freiburg, Albertstraße 21, 79104 Freiburg, Germany*
[b] *Institut für Physikalische Chemie, Universität Freiburg, Albertstraße 21, 79104 Freiburg, Germany*
[c] *Institut für Biologie 2, Universität Freiburg, Schänzlestraße 1, 79104 Freiburg, Germany*
[d] *Institut für Anorganische Chemie, Universität München, Butenandtstraße 5-13, Haus D, 81377 Munich Großhadern, Germany*

Received 28 November 2000; accepted 28 February 2001

Abstract

The optical absorption and luminescence spectra, the electrochemical behavior, and the X-ray crystal structure of a series of three heteroleptic Ru(II) complexes in comparison to $[Ru(bipy)_3]^{2+}$ are reported. The complexes examined are of the type $[Ru(bipy)_2(bipy')](PF_6)_2$ with bipy = 2,2′-bipyridine and bipy′ = 5,5′-diamino-2,2′-bipyridine (**4**), diethyl-2,2′-bipyridine-5,5′-dicarboxylate (**5**) or 5,5′-bis(ethoxycarbonylamino)-2,2′-bipyridine (**6**). Absorption bands and redox waves are fully assigned. The position of bands or half-wave potentials can be correlated with the electron-withdrawing/donating properties of the bipy′ ligand. The relative emission intensities of complexes with **4** and **6** can be modulated through the hydrogen-bonding capabilities of the solvent (MeOH and H_2O). The cyclic voltammograms between +1.5 and −2.2 V show a reversible metal-oxidation wave and two to four reduction waves, attributed to successive reductions of the different ligands. Ligand **4** can only be oxidized. Correlations between spectroscopical and electrochemical data give a linear relation for $h\nu_{max}^{abs}$, $h\nu_{max}^{em}$ versus $\Delta E_{1/2}$. A comparison with complexes with the analogous 4,4′-disubstituted-2,2′-bipyridine ligands reveals pronounced differences in the position of the MLCT-absorption and emission bands due to the 5- or 4-position of the substituent. © 2001 Elsevier Science B.V. All rights reserved.

Keywords: Bipyridine complexes; Ruthenium complexes; Luminescence; Crystal structures; Electrochemistry

1. Introduction

There is a great interest in ruthenium(II) complexes with 2,2′-biypridine (bipy), 2,2′:6′,2″-terpyridine or 1,10-phenanthroline ligands and their derivatives because of their light-induced electron and energy transfer properties [1–3]. In recent applications based on these phenomena, ruthenium compounds are designed to behave as luminescent DNA or protein probes [4–7], as model systems for electron-transfer proteins [8], and as luminescent analytic sensor systems able to detect neutral organic molecules [9,10] or inorganic cations [11–13]. Because of their properties, ruthenium(II) polypyridine compounds are incorporated into oligomers, dendrimers, and polymers [14–16]. The photochemical function can be modulated through the ligand design [17]. The majority of ruthenium(II)–bipyridine complexes has ligands that are modified in the 4 and 4′ positions (**1**) [2–5,8,13,14,18,19]. Ruthenium(II)–bipyridine compounds where the bipy-ligand is substituted in the 5,5′-position (**2**) are much rarer [6,9,12,15].

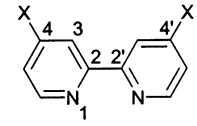

4,4′-disubstituted-2,2′-bipyridine

1

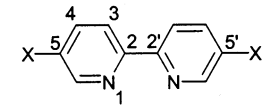

5,5′-disubstituted-2,2′-bipyridine

2

* Corresponding author. Tel.: +49-761-2036127; fax: +49-761-2036147.
E-mail address: janiak@uni-freiburg.de (C. Janiak).

0020-1693/01/$ - see front matter © 2001 Elsevier Science B.V. All rights reserved.
PII: S0020-1693(01)00414-5

We have recently set out to investigate the coordination behavior of 5,5′-disubstituted-2,2′-bipyridine ligands such as **3** [20] and **4** [21]. During the synthesis of 5,5′-diamino-2,2′-bipyridine (**4**) we isolated the intermediates diethyl-2,2′-bipyridine-5,5′-dicarboxylate (**5**) and 5,5′-bis(ethoxycarbonylamino)-2,2′-bipyridine (**6**) [21,22].

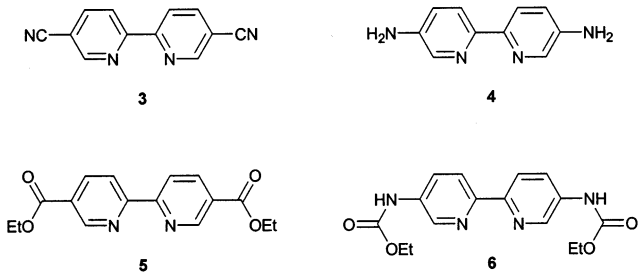

Compounds **4**–**6** form a related series of 5,5′-disubstituted bipyridines with substituents, which are useful starting groups for further derivatization and are either hydrogen-bonding donors (**4**), acceptors (**5**) or both (**6**). We report here on the synthesis of the heteroleptic complexes $[Ru(bipy)_2(bipy')](PF_6)_2$ (where bipy′ = **4**, **5** or **6**) and their comprehensive spectroscopical and electrochemical characterization.

2. Results and discussion

2.1. Synthesis

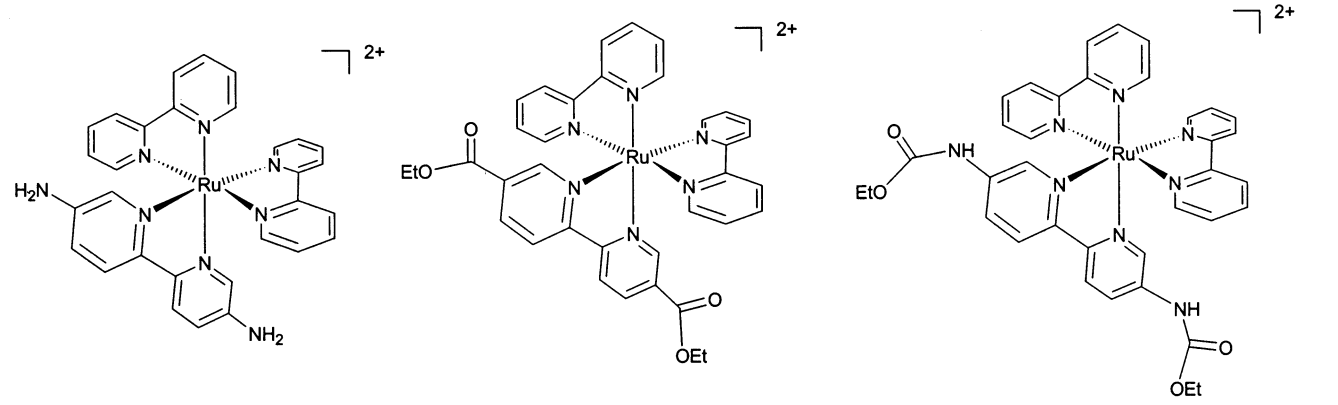

The 5,5′-disubstituted-2,2′-bipyridine ligands **4**–**6** were derived from the dimethyl bipyridine precursor, 5,5′-dimethyl-2,2′-bipyridine [21,22], which was in turn obtained through the coupling reaction of 3-methylpyridine by using a Raney–nickel catalyst [23]. Each of the ligands was purified by recrystallization. The starting material $[RuCl_2(bipy)_2]\cdot 2H_2O$ was prepared as dark-purple micro-crystalline powders by refluxing $RuCl_3\cdot xH_2O$, 2,2′-bipyridine and LiCl in DMF [24]. There are several established methods for preparing heteroleptic ruthenium(II)–bipyridine complexes, $[Ru(bipy)_2(bipy')]^{2+}$, and two of them were utilized in this work [5,25]. Reaction of the bis(bipyridine)ruthenium(II) dichloride, $[RuCl_2(bipy)_2]$ with the third bipy′ ligand, followed by addition of NH_4PF_6 gave the mixed-ligand complexes **4a**, **5a** and **6a** as the hexafluorophosphates in moderate to good yields (50–90%). In the present work the homoleptic $[Ru(bipy)_3](PF_6)_2$ complex **7** was prepared as a reference material using the procedure reported by Broomhead and Young [26], which started from $RuCl_3\cdot xH_2O$. However, it can also be obtained from $[RuCl_2(bipy)_2]\cdot 2H_2O$ by the same two-step route used for the synthesis of the above heteroleptic complexes.

The ruthenium(II) complexes are thermally stable and show no reactivity towards air or moisture, except for **4a**, which is stable in the solid state but decomposes slowly in solution after several days. The colors of the complexes varied from light orange to brown–red depending on the substituent group on the 5,5′ positions. Complex **4a** is orange–red, **5a** brown–red, and **6a** was obtained as an orange powder. The latter color is similar to the color of the reference complex $[Ru(bipy)_3](PF_6)_2$ (**7**). The red complexes **4a** and **5a** are soluble in polar organic solvents such as acetonitrile and are less soluble in CH_2Cl_2, methanol, ethanol, and water; the orange compound **6a** exhibits markedly lower solubilities in all solvents compared with **4a** and **5a**.

2.2. NMR spectroscopy

The aromatic protons in the bipyridine rings exhibit complex multiplets in the region from 6.8 to 9.1 ppm in the ^1H NMR spectra of the compounds. A notable characteristic of *cis*-ruthenium-bis(bipyridine) compounds, *cis*-$[Ru(bipy)_2(L)_2]^{2+}$, or heteroleptic ruthenium tris(bipyridine) complexes, $[Ru(bipy)_2(bipy')]^{2+}$,

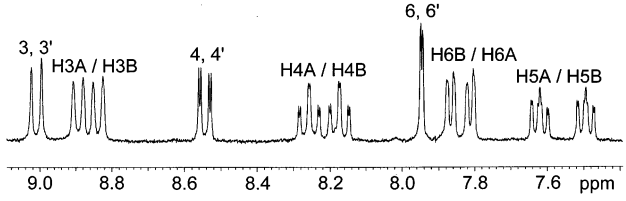

Fig. 1. The aromatic region of the ^{1}H NMR spectrum of **5a** in DMSO. For the assignment see **2** and **8**. The notation HXA/HXB refers to the unsubstituted bipy ligand, X, X′ to the 5,5′-substituted bipy′ ligand (see text).

is that each of the two pyridine rings of a given unsubstituted bipyridine unit lies in a magnetically non-equivalent position, because they are in different shielding environments [6,27]. This may already be evident from the schematic drawings for **4a**, **5a**, and **6a**. The slight difference between the shielding environments of the two pyridine rings in an unsubstituted bipyridine group can be seen more clearly in **8**.

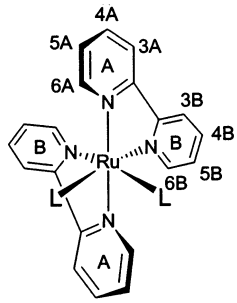

8

The pyridine ring A is *trans* to another pyridine ring A, while ring B is *trans* to an L group (substituted bipyridine). Thus, the protons on the pyridine rings A and B are magnetically non-equivalent. The C_2-symmetry operation does not relate the rings A and B. As a result there should be eight distinct signals in the ^{1}H NMR spectra for the unsubstituted bipyridine ligands. According to the coupling scheme of 2,2′-bipyridine, four of these resonances are predicted to be triplets (H4A, H4B, H5A, H5B) and the other four doublets (H3A, H3B, H6A, H6B, cf. **8**) [27]. At high enough resolutions long-range coupling leads to additional doublet-splitting on the order of 1.4–2.0 Hz. These splitting patterns are clearly seen in the ^{1}H NMR spectra of complexes **4a**, **5a**, and **6a**. The spectrum of complex **5a**, where all the signals are well separated, is given as an example in Fig. 1. It should be pointed out that the two sets of protons on the unsubstituted bipyridine ligands were identified by the symbols A and B. However, an unequivocal assignment of a set of signals to A or B could not be made. Within each set the assignment was, however, possible by a H,H COSY spectrum. If, for example, the low-field doublet of H3 was assigned to A, then the 2D-spectrum showed that H4A and H5A were also at a lower field (larger ppm value) from the respective B-protons. However, H6A would be at a higher field from H6B.

From the overall 11 signals in the aromatic region, three resonances occuring at 8.89 (d), 8.54 (dd) and 7.94 (d) ppm can be assigned to the protons in the 3,3′, 4,4′, and 6,6′ positions, respectively, of the substituted bipyridine ring. The two sets of protons for the substituted and unsubstituted pyridine rings have the correct ratio of 6:16.

In addition, there is also an interaction through space between the bipyridine rings and the groups of the substituted bipy′-ligand [6]. Part of the group lies in the shielding cone of the bipyridine ligand. In complex **5a** the CH_2-group of the ethoxy moiety does not appear as a quadruplet but as a quadruplet–doublet, in the ^{1}H NMR. Coupling to the methylene group is supplemented by either a long-range or through space coupling to hydrogen atoms of the pyridine ring. The

Table 1
Comparison of ^{1}H NMR chemical shifts (in ppm) of the pyridine ring protons in ligand **4**–**6** and ruthenium complexes **4a**–**7**

	2,2′-bipy				5,5′-disubstituted-2,2′-bipy		
	H3A,B	H4A,B	H5A,B	H6A,B	H3,3′	H4,4′	H6,6′
Bipy [a]	8.49	7.80	7.28	8.70			
7, $Ru(bipy)_3^{2+}$ [a]	8.50	8.05	7.39	7.73			
7, this work	8.82	8.16	7.52	7.72			
4					7.85	6.94	7.90
4a	8.82	8.15	7.60, 7.48	7.77, 7.68	8.04	7.09	6.86
5 [b]					8.58 [b]	8.47 [b]	9.21
5a	8.89, 8.84	8.26, 8.18	7.61, 7.49	7.87, 7.81	9.01	8.54	7.94
6					8.21	7.98	8.68
6a	8.83	8.17	7.52	7.79, 7.70	8.52	8.08	7.83

[a] Ref. [42].

[b] The correct assignment of H3 and H4, given here, is reversed from the one reported earlier in Refs. [21,22]. Furthermore, an additional ^5J-coupling between H3 and H6 is now observed for **5**: 9.21 (dd, $^4J = 2.1$, $^5J = 0.8$ Hz, H6,6′), 8.58 (dd, $^3J = 8.3$, $^5J = 0.8$ Hz, H3,3′), 8.47 (dd, $^3J = 8.2$, $^4J = 2.1$ Hz, H4,4′).

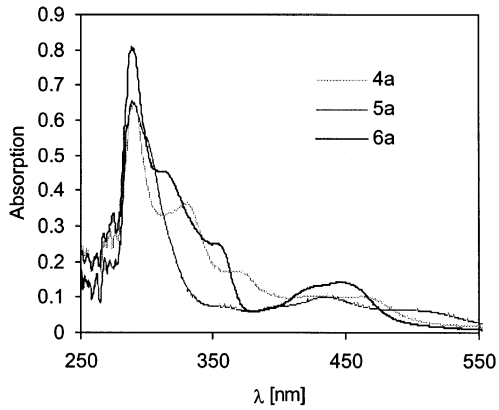

Fig. 2. Absorption (UV–Vis) spectra of compounds **4a**–**6a** in MeOH. Concentration 10^{-5} mol l^{-1}, optical path length 1 cm.

ligand alone does not show this additional doublet-splitting of the ethoxy CH_2-group in the ^1H NMR.

Table 1 shows the proton chemical shifts of the free ligands and the corresponding complexes, together with those of 2,2′-bipyridine and $[Ru(bipy)_3]^{2+}$ (**7**). The introduction of the electron-withdrawing ethoxycarbonyl group (–COOEt) onto the bipyridine ring in **5** leads to a significant downfield shift of the protons in the 4- and 6- positions in the pyridine ring. Substitution with amino groups (ligand **4**) causes an upfield shift, whereas the ring protons in **6** show very similar chemical shifts to those of 2,2′-bipyridine.

2.3. UV–Vis absorption spectra

The optical absorption spectra of the complexes show quite a number of bands (Fig. 2). Generally, the electronic transitions in ruthenium(II) tris-bipyridine complexes can be classified as metal centered (MC, d–d), ligand centered (LC, π–π*) and metal-to-ligand or ligand-to-metal charge transfer (MLCT or LMCT) [2]. In the case of heteroleptic $[Ru(bipy)_2(bipy')]^{2+}$ complexes, more excited states (ML′CT), and therefore additional absorption bands, are expected due to the different orbital energies of the different ligands [2]. Moreover, the energies of the LC bands of each ligand are usually unaffected by the other ligands. The positions of the electronic absorption maxima and the extinction coefficients for the complexes **4a**–**6a** and $[Ru(bipy)_3]^{2+}$ (**7**) are given in Table 2.

The metal-to-ligand d–π* charge transfer of the ruthenium tris(bipyridine) complexes usually occurs in the visible region between 400 and 600 nm [2]. For the mixed-ligand complexes $[Ru(bipy)_2(bipy')]^{2+}$ there should be two maxima in this region corresponding to the MLCT and ML′CT transitions, respectively. Separate charge-transfer bands have been observed in a series of mixed-ligand complexes [28]. Such features can also be seen in the absorption spectra of the complexes **4a**–**6a** (Fig. 2). We note, however, that a mixed-ligand structure is not necessary for observing two bands in the MLCT region. The absorption spectrum of $[Ru(bipy)_3]^{2+}$ shows two MLCT bands, which are close together, very similar to the spectrum of **6a**.

The lower-energy absorptions usually correspond to a promotion of the electron to the ligand easier to reduce. The ligand **4** could not be reduced by cyclic voltammetry (see below). Thus, in **4a** the lower-energy absorption is assigned to the MLCT processes involving the unsubstituted bipy ligands. The higher-energy/shorter wavelength absorption is due to the metal-to-**4**-π* charge transfer. At the same time, in **4a** we also observe a solvent dependency of some of the absorption bands. This solvent effect is most pronounced in the shift of the L′C, (**4**)π–π* bands in **4a** (Fig. 3), but is slightly evident in the lowest-energy absorption as well. The solvent dependence of CT bands is a well-known fact, and could be interpreted on the basis of solvent parameters like acceptor or donor number and solvent polarity. Here, hydrogen bonding may seem to be the most straightforward explanation in view of the known hydrogen-bonding capabilities of the amino group in **4** [21]. The irreversible reduction potential of ligand **6** is very similar to that of bipyridine (cf. Table 3). Consequently, the two maxima of the charge-transfer bands are close together and an unequivocal assignment may seem difficult. However, a careful examination based upon the correlation between spectroscopy and electrochemistry (see below) supports in both **4a** and **6a** the assignment of the lower-energy absorption to the MLCT process with L = bipy.

In an investigation of the photophysical properties of a series of $[Ru(bipy')_3]^{2+}$ complexes, where bipy′ is a 4,4′- or 5,5′-disubstituted bipyridine, it was found that the presence of electron-withdrawing substituents at the 5,5′-position led to a very substantial shift of λ_{max} to longer wavelengths [29]. Electron-donating groups caused a blue-shift (to shorter wavelengths) of λ_{max} relative to the parent system $[Ru(bipy)_3]^{2+}$. For example, $[Ru(\mathbf{5})_3]^{2+}$ showed an ML′CT absorption at 495 nm, similar to that of $[Ru(bipy)_2(\mathbf{5})]^{2+}$ (**5a**) obtained in this work. It has also been reported in the same paper that substituents, either electron-donating or withdrawing ones, at the 4,4′-position, all shifted the charge-transfer band to longer wavelengths compared with $[Ru(bipy)_3]^{2+}$.

2.4. Emission spectra

Excitation of the LC and MLCT bands of the complexes at room temperature produced emissions at longer wavelengths. The lowest-lying $ML^{(')}CT$ triplet state is responsible for the emission [30]. The emission spectra are shown in Fig. 4 and the positions of the bands are included in Table 2. Upon excitation at 450

Table 2
Spectroscopic absorption (UV–Vis) and emission data of **4a**–**7**

Complex [a]	λ_{max}^{abs} (nm)		ε [b]		Assignment	λ_{max}^{em} (nm) [c] (excitation wavelength)
	MeOH	H_2O	MeOH	H_2O		
4a	290	288	65 100	75 200	LC, bipy π–π*	626 (290)
	328	322 (sh)	36 300	34 700	L′C, **4**π–π*	
	366	354	17 600	17 600	L′C, **4**π–π*	
	425	425	10 600	10 900	ML'CT, d–(**4**)π*	
	462	454	10 300	10 700	MLCT, d–(bipy)π*	623 (450)
5a	288	288	65 500	74 900	LC, bipy π–π*	604 (290)
					and L′C, **5** π–π*	637 (290)
	299 (sh)	297 (sh)	55 000	62 200	L′C, **5** π–π*	706 (290)
	434	433	10 200	9 700	MLCT, d–(bipy)π*	
	498	495	6600	5400	ML′CT, d–(**5**)π*	702 (450)
6a	288	288	80 000	69 900	LC, bipy π–π*	602 (290)
	313	310	45 300	40 100	L′C, **6** π–π*	
	352	349 (sh)	25 100	20 000	L′C, **6** π*	
	424 (sh)	422 (sh)	12 800	11 300	ML′CT, d–(**6**)π*	
	447	448	14 200	13 300	MLCT, d–(bipy)π*	602 (450)
7	286	286	89 800	88 500	LC, bipy π–π*	
	450	453	15 700	14 900	MLCT, d–(bipy)π*	604 (450)

[a] All complexes measured at a concentration of 1×10^{-5} mol l^{-1}.
[b] In 1000 cm^2 mol^{-1} = dm^3 mol^{-1} cm^{-1}.
[c] Both in MeOH or H_2O.

nm, complex **6a** shows a broadened emission peak at 602 nm, which resembles those of the parent compound $[Ru(bipy)_3]^{2+}$ (**7**) with respect to both intensity and position. In this work, the emission of $[Ru(bipy)_3]^{2+}$ in methanol solution was observed as a broad band with a maximum at 604 nm. A collection of data verifies the emission band of $[Ru(bipy)_3]^{2+}$ in different solvents in the range of 600–630 nm [2]. Comparison of the position of the emission bands among different references is possible only if the emission spectra are corrected for detector response. Our emission spectra are not corrected. However, the detector characteristic in the wavelength region between 500 and 700 nm is rather flat, so that we do not expect a sizable shift of the band position.

The similarity in the emission properties of **6a** and $[Ru(bipy)_3]^{2+}$ is intimately related to the proximity of the charge-transfer bands of the two complexes (see above). It seems that the substituents have no effect on the absorption and emission wavelengths in complex **6a**. Such was also found for a ruthenium(II) complex with three 5,5′-bisacetamino-2,2′-bipyridine ligands (–NNCOMe), in which the emission wavelength is the same as that of $[Ru(bipy)_3]^{2+}$ [29].

Upon excitation at 450 nm, compound **4a** exhibits an emission at 623 nm with an intensity much lower than that of **6a**. It was found earlier that substitution at the 4,4′-position resulted in a red-shift of the emission band, whereas the effect of the substituents at the 5,5′-positions depended on their nature: electron-donating groups caused a blue-shift and electron-withdrawing groups a red-shift in wavelength [29]. The result for **4a**, where the amino group in **4** is electron-donating, does not adhere to this finding. This is probably due to the instability of this compound. As will be seen in the following section on the redox properties, **4a** is easy to oxidize and this may result in some changes of the orbital energy ordering, and in turn the photophysical behavior. The lowered intensity of the emission band is also a result of the instability. The third complex, **5a**, which consists of electron-withdrawing substituents at the 5,5′-positions, exhibits three emissions (after excitation at 450 nm) with the lowest energy one at 702 nm. However, their intensity is very weak compared with

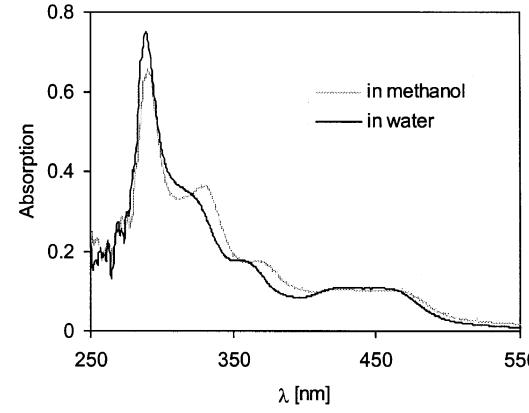

Fig. 3. Absorption (UV–Vis) spectra of **4a** in MeOH and H_2O. Concentration 10^{-5} mol l^{-1}, optical path length 1 cm.

Table 3
Half-wave potentials ($E_{1/2}$) (V) [a] at room temperature of the complexes **4a**–**7** (in acetonitrile) and the free ligands **4**–**6** and bipy (in THF)

Compound	Redox couple, n [b]					
	3+/2+	2+/1+	1+/0	0/1−	1−/2−	2−/3−
7, $[Ru(bipy)_3]n$ [b]	+1.25	−1.37	−1.55	−1.80	−2.45*	
4a	+1.06	−1.44	−1.67	−2.22*		
	+1.24 (ligand oxidation)					
5a	+1.36	−0.85	−1.25	−1.60	−1.88	−2.73*
6a	+1.24	−1.50	−1.71	−2.46*		
Ligands						
Bipy				−2.11	−2.70*	
				−2.22 [c]	−2.86* [c]	
4			+1.27 [c]			
5				−1.58	−1.93	
6				−2.12*		

[a] An asterisk indicates an irreversible reduction. The value then given is the cathodic peak potential, E_{pc}, calibrated with ferrocene (+0.352 V vs Ag/AgCl).
[b] n is the overall charge of the compounds.
[c] In acetonitrile.

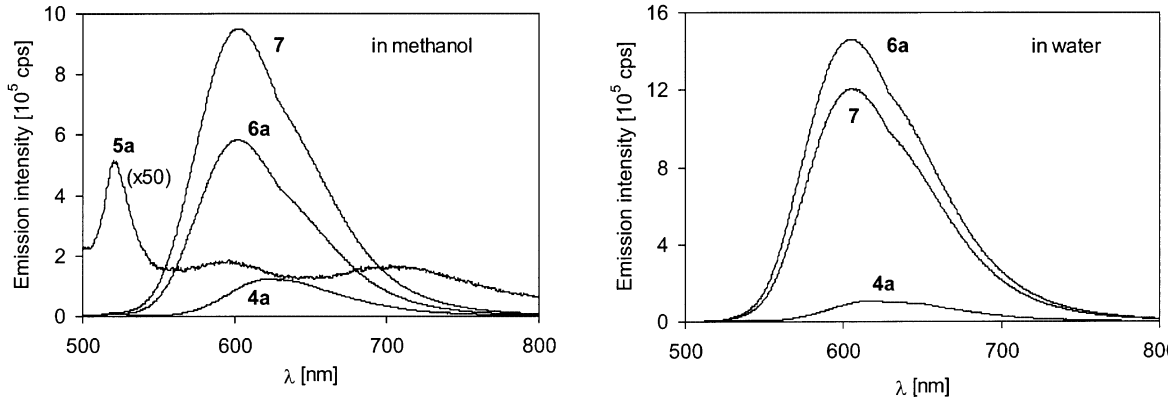

Fig. 4. Solvent-dependency of the emission intensity for **4a**–**7** at an excitation wavelength of 450 nm (in counts per second, cps). Spectra in methanol (left) and water (right). Concentration 10^{-5} mol l^{-1}, optical path length 1 cm. The weak intensity of the spectrum of **5a** has been multiplied by a factor of 50.

the other complexes and they could hardly be observed, so that the bands are not visible on the scale of Fig. 4. We know that mononuclear Ru(II) polypyridine complexes feature as a rule a single emission band. The three bands exhibited by complex **5a** could be due to an instrumental artifact, or to the presence of impurities. We will further investigate the origin of the three emission lines. However, their very low intensities may make an unequivocal assignment impossible. The excitation spectra of all the complexes have been measured and agree with the absorption spectra.

Excitation at 290 nm (spectra not shown) again produces the strongest emission for compound **6a** (in MeOH) at 602 nm. The emission intensity of complex **4a** at 626 nm is less than half of that of **6a**. Compound **5a** shows again only very weak emission bands at 604, 637, and 706 nm.

The emission intensity is solvent-dependent. In MeOH the emission from $[Ru(bipy)_3]^{2+}$ (**7**) is more intense than that of **6a** by a factor of approximately 1.5. In H_2O the emission of **6a** becomes more intense over the one of **7** by a factor of 1.25. The emission intensity of **4a** is only about 25% (7%) of that of **6a** in MeOH (H_2O). Fig. 4 illustrates the solvent-dependency of the emission intensity. The relative emission intensity in different solvents can be compared because the absorbance at the excitation wavelength of 450 nm is essentially the same in water and methanol, as can be seen from Fig. 3 and Table 2.

2.5. Electrochemistry

The redox properties of the complexes presented here differ substantially from each other. They are strongly dependent on the substituents of the bipy′ ligand. Cyclic voltammograms of acetonitrile solutions of the complexes are shown in Fig. 5, and the corresponding half-wave potentials, together with those of the free

ligands, are listed in Table 3. It is well-known that the electrochemical behavior of the ruthenium(II) polypyridyl complexes is usually observed as a metal-centered oxidation and a series of ligand-centered reductions [31]. The parent and reference complex $[Ru(bipy)_3]^{2+}$ exhibits three reversible one-electron reductions to give $[Ru(II)(bipy^{1-})_3]^-$ [2].[1] Such reduction waves were also reproduced in this work. For the complexes **4a**–**6a**, however, there are different patterns in both the oxidation and the reduction regions. The cyclic voltammogram of compound **5a** (Fig. 5(b)) contains one reversible oxidation wave and four reversible reductions. The first and second of these reductions occur at more positive potentials relative to the first reduction of the reference complex $[Ru(bipy)_3]^{2+}$. Compound **6a** (Fig. 5(c)) exhibits one oxidation and two reductions while **4a** (Fig. 5(a)) shows two oxidations and two reductions.

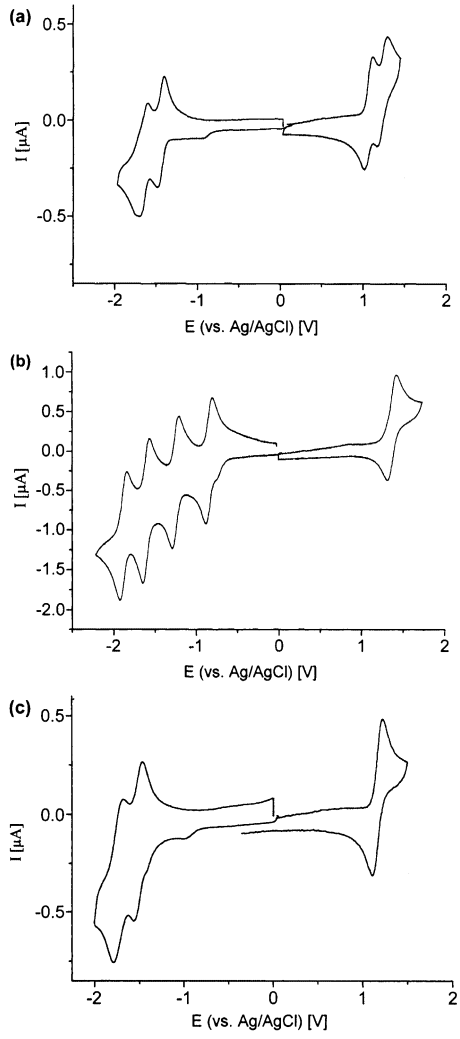

Fig. 5. Cyclic voltammograms for the reversible oxidation and reduction waves of: (a) **4a**; (b) **5a**; and (c) **6a** in acetonitrile (complex concentration 10^{-3} mol l^{-1}, 25°C, scan rate 100 mV s^{-1}, 0.1 mol l^{-1} $[n\mathrm{Bu}_4\mathrm{N}]\mathrm{PF}_6$).

Oxidation usually involves a metal-centered π-orbital and a Ru(III) complex is thereby formed. In comparison with $[Ru(bipy)_3]^{2+}$ (+1.25 V), the metal-centered oxidation potential of **5a** (+1.36 V) is slightly more positive, whereas that of **4a** (the first oxidation wave +1.06 V) is significantly less positive and that of **6a** (+1.24 V) is very close to the reference. These results can be understood considering the nature of the substituted ligands. The ruthenium oxidation potential is affected by the nature of the ligands. For closely related ligands, such as substituted bipyridines, electron-withdrawing groups increase the oxidation potential; electron-releasing groups decrease the oxidation potential. The presence of electron-withdrawing substituents on the bipyridine rings stabilizes the low Ru(II) oxidation state and the electron-donating groups favor the higher Ru(III) state in the ruthenium polypyridine family [32,33]. The ethoxycarbonyl group serves as a strong electron-withdrawing group; thus, the Ru(II) in **5a** is more difficult to oxidize and the oxidation appears at more positive potentials. It is reported that the complex $[Ru(\mathbf{5})_3]^{2+}$ shows an oxidation at a further positive potential (+1.53 V) [33]. The weak electron-donating group –NHCOOEt has no considerable effect on the oxidation behavior of the complex **6a**. The case in **4a** is somewhat complicated: Two oxidation waves are observable, with the first one at a considerably lower potential (+1.06 V) than is typical for the Ru(II) oxidation. Yet, probably, this first process is due to Ru oxidation, consistent with the fact that electron-donor ligand **4** facilitates Ru oxidation with respect to the same process in $[Ru(bipy)_3]^{2+}$. The second process (+1.24) may be ligand oxidation, even if we had expected a more positive potential for oxidation of the coordinated ligand, with respect to the free ligand. This ligand can easily be oxidized, as confirmed by the redox potentials of the free ligands shown in Table 3. For the spectroscopic and redox correlations in Table 4 and Fig. 6, we have calculated with the process at +1.06 for the Ru oxidation potential $E_{1/2}(3+/2+)$. The good correlation coefficient for the straight line may be viewed as an indication of correct assignment. It should be pointed out that **4a** is unstable in solutions, as mentioned in Section 2.1, and the ligand **4** is also sensitive to air both in the solid state and in solution. The poor stability of **4** and **4a** can thus be traced to an oxidation of the ligand.

Reduction may involve a metal-centered or a ligand-centered orbital, depending on the relative energy ordering. For $Ru(bipy)_3$ complexes, reduction commonly takes place on a ligand π*-orbital. Thus, the reduced form usually still has a Ru(II) center with a low-spin d^6-configuration. The bipyridine substituents also affect

[1] Under special conditions up to six electrons can be pumped into $[Ru(bipy)_3]^{2+}$ to give $[Ru(II)(bipy^{2-})_3]^{4-}$, see Ref. [35].

Table 4
Spectroscopic data and redox energies ($\Delta E_{1/2}$) of the Ru(II) complexes

Compound	L [a]	λ_{max}^{abs} (nm) [b]	$h\nu_{max}^{abs}$ (eV) [c]	λ_{max}^{em} (nm) [d]	$h\nu_{max}^{em}$ (eV) [c]	$\Delta E_{1/2}$ (eV) [e]
7, $[Ru(bipy)_3]^{2+}$	bipy	450	2.76	604	2.05	2.62
4a	bipy	462	2.68	623	1.99	2.50
5a	**5**	498	2.49	702	1.76	2.20
6a	bipy	447	2.77	602	2.06	2.74

[a] L = relevant ligand for the lowest-energy absorption/emission process and the first reduction wave.
[b] From Table 2, values for $ML^{(\prime)}CT$ in MeOH.
[c] $h\nu = hc/\lambda$; $hc = 1239.82$ eV nm.
[d] See Section 2.4; excitation at 450 nm in MeOH.
[e] $\Delta E_{1/2} = e[E_{1/2}(3+/2+) - E_{1/2}(2+/1+)]$; for the half-wave potentials, see Table 3.

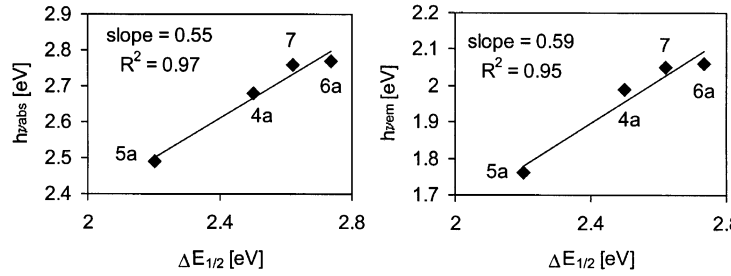

Fig. 6. Correlations between the redox energy ($\Delta E_{1/2}$) and the energy of the $ML^{(\prime)}CT$ absorption (left) and emission (right) maxima for the complexes **4a**–**7**.

the reduction behavior of the ruthenium(II) complexes. The presence of the electron-withdrawing ligands often leads to additional reduction waves of the ruthenium complexes. For example, the ruthenium complexes with three 5,5′- or 4,4′-diethoxycarbonyl-2,2′-bipyridine ligands exhibit six reversible reductions [33] or even more (up to 10 waves) at reduced temperatures [34]. Here, the complex **5a** contains only one substituted ligand and correspondingly, four reduction waves were observed. It is noteworthy that the reduction processes of (heteroleptic) ruthenium-bipyridine compounds are usually explained by a 'localization model' [30]. That is, each of the reduction steps can be attributed to one or several definite ligands, i.e. the additional electron is localized on a specific ligand, and delocalization is considered negligible.

The ground-state reduction potential of the complex can be roughly related to the reduction potential of the free ligand, because the same π*-LUMO is involved. Mixed-ligand complexes allow for a clearer localization of the acceptor orbitals in the reduction process if the different bipyridine ligands have different energies of the π*-orbitals. It can be seen from Table 3 that the free ligand **5** shows two reductions [33] occurring at less negative potentials (−1.58 and −1.93 V) than that of the unsubstituted bipyridine ligand (−2.11 V). Hence, the first and second reductions of the corresponding complex **5a** (−0.85 and −1.25 V), which occur more easily than the first reduction step of $[Ru(bipy)_3]^{2+}$ (−1.37 V), can be considered localized on the substituted ligand **5**. The two remaining reduction waves, which are at similar potentials to the second and third reduction of $[Ru(bipy)_3]^{2+}$, are then due to the bipy ligands. In the cases of **4a** and **6a**, the two reversible reduction waves in each complex must be assigned to the reduction of the unsubstituted bipy ligands, since no reversible reductions were observed for the free ligands **4** and **6**.

2.6. Spectroscopic and electrochemical correlation

There are correlations between the electrochemical and the spectroscopic data. Based on Koopmans' theorem [35] the orbitals that are involved in the reduction process are the same orbitals that are involved in the MLCT transitions. There should be a linear correlation between the energies of the absorption and emission maxima for $ML^{(\prime)}CT$ and the redox energy involving the $L^{(\prime)}$ ligand [2,30,36]. Typical energy values ($h\nu$) for the maximum of the MLCT-absorption lie between 2.2 and 2.8 eV; for the emission, between 1.4 and 2.2 eV. The so-called 'redox energy', $\Delta E_{1/2}$, is given by $e[E_{1/2}(3+/2+) - E_{1/2}(2+/1+)]$, i.e. as the difference between the half-wave potentials of the oxidation and first reduction waves [2]. The relevant data are collected in Table 4. The plots of $h\nu_{max}^{abs}$ and $h\nu_{max}^{em}$ versus $\Delta E_{1/2}$ are shown in Fig. 6. In **4a** and **6a** the first reduction waves were clearly assigned to the unsubstituted bipy ligand. The linear relations for $[Ru(bipy)_2(bipy')]^{2+}$-complexes confirm the UV–Vis spectroscopic assignments of the

Table 5
Comparison of ruthenium complexes with 4,4′- and 5,5′-disubstituted-2,2′-bipyridine ligands

Compound [a]	ML′CT [b]			$E_{1/2}$ of the redox couple [c] (V)					Ref.
	λ_{max}^{abs} (nm)	ε	λ_{max}^{em} (nm)	3+/2+	2+/1+	1+/0	0/1−	1−/2−	
4a = $[Ru(bipy)_2(5,5'\text{-diNH}_2\text{-bipy})]^{2+}$	462 (in MeOH)	10 300	623						
$[Ru(4,4'\text{-diNH}_2\text{-bipy})_3]^{2+}$	504 (in EtOH–MeOH)	10 500	705						[29]
5a = $[Ru(bipy)_2(5,5'\text{-diCO}_2\text{Et-bipy})]^{2+}$	498 (in MeOH)	6600	702	+1.36 (in MeCN)	−0.85	−1.25	−1.60	−1.88	
$[Ru(4,4'\text{-diCO}_2\text{Et-bipy})_3]^{2+}$	464 (in EtOH–MeOH)	23 300	655						[29]
$[Ru(bipy)_2(4,4'\text{-diCO}_2\text{Et-bipy})]^{2+}$	~480 (in H_2O)								[41]
				+1.38 (in DMF)	−0.93	−1.36	−1.56	−1.90	[33]
				+1.32	−0.96				[41]

[a] bipy = 2,2′-bipyridine.
[b] Metal-to-ligand charge transfer involving the substituted 4,4′- or 5,5′-bipyridine ligand. Data from Table 2.
[c] Data from Table 3 for complexes reported in this work.

lowest accepting (π*) orbitals of the complexes to bipy in the case of **4a** and **6a** and to bipy′ for **5a** [36]. Using $h\nu_{max}$ of the second lowest-absorption would put the data points for **4a** and **6a** off the connecting line between **5a** and **7**. Thus, the lowest-energy MLCT-absorption in **4a** and **6a**, respectively, involves the unsubstituted bipy-ligand. The higher lying π*-orbitals of ligands **4** and **6** can be traced to their electron-donating $-NH_2$ and –NHCOOEt groups.

Data for comparison are available for selected complexes with 4,4′-disubstituted-2,2′-bipyridine ligands. The data are summarized in Table 5. The comparison reveals pronounced differences in the position of the MLCT-absorption and -emission bands upon the position of the substituent. For the amino group the bands are shifted to longer wavelengths when going from the 5- to the 4- position, whereas for the ethoxycarbonyl group the bands are shifted to shorter wavelengths for the same change from the 5- to the 4-position. The electrochemical data for complexes with the diethoxycarbonyl-substituted bipyridine indicate little effect on the oxidation potential of the metal center. The 5,5′-substituted ligand **5** is, however, somewhat easier to reduce than its 4,4′-substituted analog [33]. A direct comparison of oxidation potentials from the literature on an absolute scale (−0.85 and −1.25 versus −0.93 and −1.36) is not feasible [2]. Data for a 4,4′-substituted analog of the 5,5′-bis(ethoxycarbonylamino)-substituted bipyridine **6** or its complex **6a** were not found. To the best of our knowledge the ligand **6** has not been utilized in ruthenium chemistry.

2.7. X-ray structures of 4a–6a

The single-crystal structures of complexes **4a**–**6a** were determined to check for hydrogen bonding of the functional substituents [21] and π-stacking interactions of the aromatic nitrogen-containing ligands [37]. The molecular ruthenium tris-ligand structure of the three compounds is as expected. Fig. 7 illustrates the cation of **6a** as an example. Bond distances and angles for the three compounds are summarized in Table 6. It can be noted that the Ru–N(5,5′-bipy′) contacts lie either to the long end (in **4a** and **6a**) or to the short end (in **5a**) of the Ru–N bond lengths.

Only complexes **4a** and **5a** crystallize, with two and one molecule of methanol, respectively. Classic hydrogen bonds (Table 7) are observed in **4a** and **6a**, mainly between the N–H functionalities and the fluorine atoms of the PF_6 anions. No classic hydrogen bridges were found in compound **5a**·CH_3OH, not even involving the solvent molecule. Weak C–H···F/O/N bonds [38] are present in all three compounds. The presence of hydrogen-bonding interactions in **4a** and **6a** helps to explain the observed solvent effects on the emission intensity (see above).

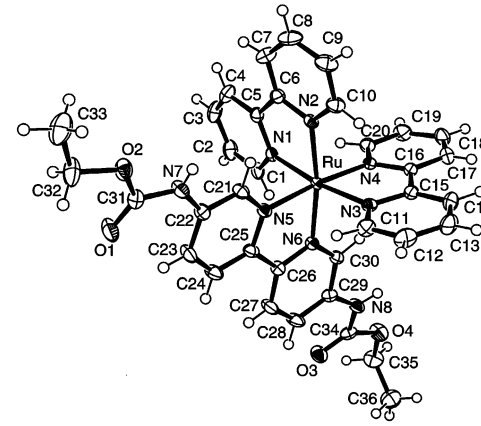

Fig. 7. Molecular structure of the $[Ru(bipy)_2(\mathbf{6})]^{2+}$ cation in **6a**.

Table 6
Selected bond lengths and angles around ruthenium in **4a**–**6a**

	4a	**5a**	**6a**
Ru–N(bipy) (Å)	2.042(4), 2.052(4), 2.055(4), 2.058(4)	2.054(3), 2.055(4), 2.055(4), 2.055(4)	2.047(2), 2.052(2), 2.060(2), 2.060(2)
Ru–N(5,5′-bipy′)	2.058(4), 2.062(4)	2.048(4), 2.050(3)	2.068(2), 2.069(2)
N–Ru–N chelate bite angles (°) [a]	78.69(17), 78.86(17), 79.08(16)*	78.59(15), 78.67(15)*, 79.07(15)	78.41(8), 78.95(9), 79.44(9)*
N–Ru–N *cis*, except chelate, range (°)	85.74(17)–99.83(17)	88.95(14)–96.56(14)	87.52(9)–98.11(9)
Average N–Ru–N *cis*,except chelate (°)	93.78	93.90	93.83
N–Ru–N *trans* (°)	172.85(16), 174.99(17), 175.92(16)	170.69(15), 172.35(14), 172.97(15)	170.85(8), 171.78(8), 174.64(8)

[a] An asterisk indicates the chelate bite angle of the 5,5′-bipy′ ligand.

Table 7
Classic hydrogen-bonding interactions in **4a**·2CH_3OH and in **6a**

Compound	D−H···A [symmetry operation]	D–H (Å)	H···A (Å)	D···A (Å)	D−H···A (°)
4a·2CH_3OH [a]	O(1)−H(81)···O(2) [1564]	0.840	1.943	2.779	174.0
	O(2)−H(82)···F(1) [2656]	0.840	2.216	3.020	160.4
	N(7)−H(771)···F(3*A*) [2666]	0.888	2.443	3.190	142.0
	N(7)−H(772)···F(9*A*) [2666]	0.933	2.542	3.435	160.4
	N(8)−H(781)···F(3A) [2665]	0.948	2.492	3.295	142.5
6a [b]	N(7)−H(71)···F(10) [2555]	0.722	2.516	2.961	121.8
	N(7)−H(71)···F(6) [4454]	0.722	2.415	3.045	146.8
	N(8)−H(81)···O(1) [4554]	0.794	2.251	2.921	142.4

[a] Symmetry equivalent positions: [1564] = x, $1+y$, $-1+z$; [2656] = $1-x$, $-y$, $1-z$; [2666] = $1-x$, $1-y$, $1-z$; [2665] = $1-x$, $1-y$, $-z$.
[b] Symmetry equivalent positions: [2555] = $0.5-x$, $0.5+y$, $0.5-z$; [4454] = $-0.5+x$, $0.5-y$, $-0.5+z$; [4554] = $0.5+x$, $0.5-y$, $-0.5+z$.

π-Stacking interactions are negligible in all three complexes. While the π-planes of the pyridine rings still have the appropriate separation of 3.5–3.6 Å, they are parallel displaced and overlap only to a small extent. The lateral shift of the ring centroid or the displacement angle is rather large [37]. In **4a** and **6a**, only the rims of the bipyridine ligands are in contact. In **5a** pyridine rings were found to stack in a graphite-like fashion with one ring atom almost over the center of the other ring.

3. Summary

The optical absorption and luminescence spectra, the electrochemical behavior and the X-ray crystal structure of a series of three heteroleptic Ru(II) complexes of the type $[Ru(bipy)_2(bipy')]^{2+}$ with bipy = 2,2′-bipyridine and bipy′ = 5,5′-disubstituted-2,2′-bipyridine are reported and fully interpreted. The relative emission intensities of complexes with bipy′ = 5,5′-bis(ethoxycarbonylamino)-2,2′-bipyridine (**6**) can be modulated through the hydrogen-bonding capabilities of the solvent. In the better hydrogen-bonding solvent H_2O, an enhancement of intensity is observed compared with a methanol solution. It was found that the ligand **4** can only be oxidized, whereas cyclic voltammetry normally allows reversible reduction of bipyridine-type ligands.

4. Experimental

$RuCl_3 \cdot xH_2O$, 2,2′-bipyridine, 3-methylpyridine, and NH_4PF_6 were purchased from ACROS and used as received. Other solvents and reagents were reagent grade or better and used without further purification. ^1H NMR spectra were recorded on a Varian O-300 (300.1 MHz) spectrometer in DMSO-d_6. UV–Vis (absorption) spectra were taken in methanol or aqueous solution with a Shimadzu UV-2101 PC Scanning Spectrophotometer. IR spectra were recorded on a Perkin–Elmer 783 infrared spectrophotometer as KBr disks. Elemental analyses were carried out with a Perkin–Elmer elemental analyzer E 240 C.

4.1. Syntheses

$[RuCl_2(bipy)_2] \cdot 2H_2O$ [24], $[Ru(bipy)_3](PF_6)_2$ [26], and the ligands 5,5′-diaminobipyridine (**4**), diethyl-2,2′-bipyridine-5,5′-dicarboxylate (**5**), and 5,5′-bis(ethoxycarbonylamino)-2,2′-bipyridine (**6**) [21,22] were prepared according to literature methods. The het-

eroleptic ruthenium(II) complexes $[Ru(bipy)_2(bipy')](PF_6)_2$ were synthesized by the published procedures as follows.

4.1.1. [Ru(bipy)$_2$(**4**)](PF$_6$)$_2$ (**4a**)

$[RuCl_2(bipy)_2]\cdot 2H_2O$ (0.150 g, 0.288 mmol) and **4** (0.067 g, 0.30 mmol) were refluxed in 70% ethanol/H_2O (25 ml) under argon for 8 h. Ethanol was removed under vacuum. After standing for 2 h, the mixture was filtered and an aqueous saturated NH_4PF_6 solution was then added to the filtrate until no further precipitate was observed. The mixture was kept at room temperature (r.t.) for 4 h and the powders were collected by filtration. The orange–red powder thus obtained was washed with cold water and diethyl ether, and dried overnight. Yield: 0.23g (90%). Single crystals of the dimethanol adduct were obtained by slow diffusion of diethyl ether into a MeOH solution of the complex. ^{1}H NMR (DMSO-d_6, δ ppm): 8.82 (t, 4H, $J = 8.2$ Hz, H3A, H3B); 8.15 (m, 4H, H4A, H4B); 8.04 (d, 2H, $J = 9.0$ Hz, H3, H3′); 7.77 (d, 2H, $J = 4.4$ Hz, H6B); 7.68 (d, 2H, $J = 4.4$ Hz, H6A); 7.60 (m, 2H, H5B); 7.48 (m, 2H, H5A); 7.09 (dd, 2H, $J_1 = 9.0$, $J_2 = 2.4$ Hz, H4, H4′); 6.86 (d, 2H, $J = 2.4$ Hz, H6, H6′); 5.94 (s, 4H, NH_2). IR (KBr, cm^{-1}): ν 3468 w, 3384 w, 1634 m, 1602 m, 1578 w, 1487 m, 1465 w, 1315 w, 1264 w, 1161 w, 842 s, 762 w, 731 w, 558 m. *Anal.* Found: C, 40.03; H, 2.75; N, 12.43. Calc. for $C_{30}H_{26}F_{12}N_8P_2Ru$ (889.6): C, 40.51; H, 2.95; N, 12.60%.

4.1.2. [Ru(bipy)$_2$(**5**)](PF$_6$)$_2$ (**5a**)

$[RuCl_2(bipy)_2]\cdot 2H_2O$ (0.15 g, 0.29 mmol) and **5** (0.09 g, 0.3 mmol) were heated at reflux in 30 ml of ethanol for 4 h. Water (20 ml) and an excess of NH_4PF_6 were added until the product was completely precipitated. The mixture was then stored in the refrigerator overnight. The brown–red solid formed was filtered, washed carefully with cold water and then diethyl ether to remove the un-reacted ligand, and dried by suction. Yield: 0.15 g (52%). Single crystals were grown from methanol solution. ^{1}H NMR (DMSO-d_6, δ ppm): 9.01 (d, 2H, $J = 8.5$ Hz, H3, H3′); 8.89 (d, 2H, $J = 8.1$ Hz, H3A); 8.84 (d, 2H, $J = 8.1$ Hz, H3B); 8.54 (dd, 2H, $J_1 = 8.5$, $J_2 = 1.8$ Hz, H4, H4′); 8.26 (td, 2H, $J_1 = 8.0$, $J_2 = 7.8$, $J_3 = 1.4$ Hz, H4A); 8.18 (td, 2H, $J_1 = 8.0$, $J_2 = 7.8$, $J_3 = 1.4$ Hz, H4B); 7.94 (d, 2H, $J = 1.5$ Hz, H6, H6′); 7.87 (d, 2H, $J = 5.6$ Hz, H6B); 7.81 (d, 2H, $J = 5.9$ Hz, H6A); 7.61 (td, 2H, $J_1 = 7.4$, $J_2 = 5.8$, $J_3 = 1.1$ Hz, H5A); 7.49 (td, 2H, $J_1 = 7.5$, $J_2 = 5.6$, $J_3 = 1.2$ Hz, H5B); 4.22 (qd, 4H, $J_1 = 7.1$, $J_2 = 1.2$ Hz, CH_2CH_3); 1.19 (t, 6H, $J = 7.1$ Hz, CH_2CH_3). IR (KBr, cm^{-1}): ν 3433.4 w, br, 3090 w, 2988 w, 1726 s, 1603 m, 1577 m, 1466 m, 1447 m, 1399 m, 1371 m, 1292 s, 1122 m, 1013 w, 839 s, 756 m, 732 w, 557 s. *Anal.* Found: C, 42.50; H, 3.14; N, 8.34. Calc. for $C_{36}H_{32}F_{12}N_6O_4P_2Ru$ (1003.7): C, 43.08; H, 3.21; N, 8.37%.

4.1.3. [Ru(bipy)$_2$(**6**)](PF$_6$)$_2$ [**6a**]

$[RuCl_2(bipy)_2]\cdot 2H_2O$ (0.150 g, 0.288 mmol) and **6** (0.096 g, 0.29 mmol) were refluxed in 70% ethanol/H_2O (25 ml) under argon for 8 h. Ethanol was removed under vacuum. After standing for 2 h, the mixture was filtered and a saturated NH_4PF_6 solution was then added to the filtrate until no further precipitate was observed. The mixture was kept at r.t. for 4 h and the powders were collected by filtration. The orange solid thus obtained was washed with cold water and diethyl ether, and dried overnight. Yield: 0.23g (77%). Single crystals of the methanol adduct were obtained by slow diffusion of diethyl ether into a MeOH/CH_3CN mixed solution. ^{1}H NMR (DMSO-d_6, δ ppm): 10.19 (s, 2H, $NHCO_2C_2H_5$); 8.83 (d, 4H, $J = 8.1$ Hz, H3A, H3B); 8.52 (d, 2H, $J = 9.1$ Hz, H3, H3′); 8.17 (m, 4H, H4A, H4B); 8.08 (dd, 2H, $J_1 = 9.0$, $J_2 = 2.2$ Hz, H4, H4′); 7.83 (d, 2H, $J = 2.1$ Hz, H6, H6′); 7.79 (d, 2H, $J = 4.7$ Hz, H6B); 7.70 (d, 2H, $J = 4.9$ Hz, H6A); 7.52 (m, 4H, H5A, H5B); 4.05 (q, 4H, $J = 7.1$ Hz, CH_2CH_3); 1.20 (t, 6H, $J = 7.1$ Hz, CH_2CH_3). IR (KBr, cm^{-1}): ν 3398 br, 3120 w, 2990 w, 1731 m, 1608 m, 1536 m, 1486 m, 1466 w, 1447 w, 1384 w, 1258 sh, 1213 s, 1080 w, 1051 w, 840 s, 764 m, 731 w, 557 m. *Anal.* Found: C, 41.93; H, 3.02; N, 10.93. Calc. for $C_{36}H_{34}F_{12}N_8O_4P_2Ru$ (1033.7): C, 41.83; H, 3.32; N, 10.84%.

4.2. Fluorescence spectra

Emission and excitation spectra were taken on a Jobin Yvon (Instruments S.A.) Fluoromax 2 spectrometer. For emission spectra the sample was excited at the indicated wavelength with a spectral bandwidth of 10 nm. Fluorescence emission was detected at an angle of 90° relative to the excitation light with a spectral bandwidth of 2 nm. Wavelength calibration of the excitation and emission monochromators was done using the spectrum of the internal Xe-lamp and a Raman spectrum, respectively.

4.3. Electrochemical measurements

All electrochemical experiments were carried out in specially constructed cells containing an internal drying column with highly activated alumina. The working electrode was a Pt disk sealed in soft glass (1.00 mm diameter). A Pt wire, wrapped around the glass of the working electrode, was used as the counter electrode. The reference electrode was an Ag wire on which AgCl had been deposited electrolytically. Potentials were calibrated with ferrocene (+0.352 V vs Ag/AgCl). The measurements were performed with a Jaissle Potentiostat IMP 88 and a PAR 175 programmer.

4.4. X-ray structure determinations

Data were collected with Mo Kα radiation ($\lambda = 0.71073$ Å) and the use of a graphite monochromator. Structure solution was performed by direct methods using SIR97 [39]. Refinement: full-matrix least-squares on F^2 [SHELXL-97 (version 97-2)] [40]; all non-hydrogen positions found and refined with anisotropic temperature factors.

The hydrogen atoms were refined as follows. In **4a** and **5a**, C-bonded H — riding with U(H) = 1.2*U(C) for CH_2 and CH, 1.5*U(C) for CH_3; N-bonded H — free refinement; O-bonded H — the position of the O-bonded H of the methanol molecule was refined with respect to a staggered conformation and a possible or bridge, U(H) = 1.5*U(O). In **6a** all hydrogen atoms were found and fully refined, including temperature factors.

In **4a** one PF_6 molecule was disordered. The disorder can be described by a rotation (rotation axis F1–P–F6). The best fit for the electron density around the second PF_6 molecule succeeds in assuming three possible positions for it. The geometry is constrained to an undisturbed part of the first PF_6 molecule. The two molecules with the smaller s.o.f.s are refined with one common temperature factor each. In **5a** the C–O-distance of the methanol molecule must be fixed.

Crystal data are listed in Table 8. Graphics were computed with ORTEP3 for Windows [41].

5. Supplementary material

Crystallographic data (excluding structure factors) for the structural analysis have been deposited with the Cambridge Crystallographic Data Center, CCDC Nos.

Table 8
Crystal data for compounds **4a**–**6a**

Compound	**4a**·2CH_3OH	**5a**·CH_3OH	**6a**
Empirical formula	$C_{32}H_{34}F_{12}N_8O_2P_2Ru$	$C_{37}H_{36}F_{12}N_6O_5P_2Ru$	$C_{36}H_{34}F_{12}N_8O_4P_2Ru$
M (g mol^{-1})	953.66	1035.72	1033.70
Crystal size (mm)	0.25 × 0.12 × 0.08	0.35 × 0.20 × 0.10	0.30 × 0.10 × 0.03
Crystal description	prismatic	prismatic	platelet
Crystal color	brown	brown	red
Temperature (K)	200(3)	200(3)	200(3)
Diffractometer	STOE-IPDS	STOE-IPDS	STOE-IPDS
Scan type, 2θ range (°)	ω, 3.6–51.7	ω, 3.4–47.9	ω, 3.8–51.8
h, k, l range	−14, 14; −15, 15; −15, 16	−16, 16; −24, 23; −15, 13	−13, 13; −25, 26; −19, 19
Crystal system	triclinic	monoclinic	monoclinic
Space group	P-1	$P2_1/c$	$P2_1/n$
Unit cell dimensions			
a (Å)	12.1279(11)	14.2786(9)	11,5936(6)
b (Å)	12.7038(11)	21.1701(15)	21.6143(16)
c (Å)	13.5898(11)	13.6299(9)	15.9556(10)
α (°)	77.408(10)	90	90
β (°)	89.388(10)	96.622(8)	97.963(7)
γ (°)	67.086(10)	90	90
V (Å^3)	1875.8(3)	4094.1(5)	3960.3(4)
Z	2	4	4
D_{calc} (g cm^{-3})	1.6885(3)	1.6803(2)	1.73374(18)
F(000)	960	2088	2080
Absorption coefficient (mm^{-1})	0.607	0.567	0.586
Absorption correction	numerical	numerical	numerical
Min/max transmission	0.890/0.960	0.843/0.947	0.9345/0.9826
Measured reflections	13 292	16 643	22 727
Independent reflectections	6772 [$R_{int} = 0.0356$]	6345 [$R_{int} = 0.0559$]	7195 [$R_{int} = 0.0420$]
Observed reflections [$I > 2\sigma(I)$]	5203	4415	4829
Parameters refined	541	571	704
Max/min $\Delta\rho \cong$ [a] (e Å^{-3})	1.210/−0.894	0.672/−0.699	0.325/−0.406
R_1/wR_2 [b] [$I > 2\sigma(I)$]	0.0591/0.1576	0.0464/0.1040	0.0278/0.0542
R_1/wR_2 [b] (all reflections)	0.0774/0.1673	0.0741/0.1112	0.0542/0.0582
Goodness-of-fit on F^2 [c]	1.044	0.918	0.846
Weighting scheme w; a/b [d]	0.1132/0.000	0.0653/0.000	0.0269/0.0000

[a] Largest difference peak and hole.
[b] $R_1 = (\Sigma||F_o| - |F_c||)/\Sigma|F_o|$; $wR_2 = [\Sigma[w(F_o^2 - F_c^2)^2]/\Sigma[w(F_o^2)^2]]^{1/2}$.
[c] Goodness-of-fit $= [\Sigma[w(F_o^2 - F_c^2)^2]/(n-p)]^{1/2}$.
[d] $w = 1/[\sigma^2(F_o^2) + (aP)^2 + bP]$ where $P = (\max(F_o^2 \text{ or } 0) + 2F_c^2)/3$.

150781–150783 for **4a**·2CH_3OH, **5a**·CH_3OH, and **6a**, respectively. Copies of this information can be obtained free of charge from The Director, CCDC, 12 Union Road, Cambridge CB2 1EZ, UK (fax: +44-1223-336033; e-mail: deposit@ccdc.cam.ac.uk or www: http://www.ccdc.cam.ac.uk).

Acknowledgements

This work was supported by the Deutsche Forschungsgemeinschaft (grant Ja466/10-1), the Wissenschaftliche Gesellschaft in Freiburg, the Graduate College 'Unpaired Electrons' at the University of Freiburg, and the Fonds der Chemischen Industrie. We gratefully acknowledge a generous gift of $RuCl_3 \cdot xH_2O$ from Degussa-Hüls AG. Support by Professor W. Haehnel and Mrs. Ottilie Thorwarth is greatly appreciated. One of the referees is thanked for his valuable comments.

References

[1] (a) K. Kalyanasundaram, in: K. Kalyanasundaram, M. Grätzel (Eds.), Photosensitization, Photocatalysis using Inorganic and Organometallic Compounds , Kluwer Academic Publishers, Dordrecht, 1993. (b) M. Yanagida, L.P. Singh, K. Sayama, K. Hara, R. Katoh, A. Islam, H. Sugihara, H. Arakawa, M.K. Nazeeruddin, M. Grätzel, J. Chem. Soc., Dalton Trans. (2000) 2817.

[2] A. Juris, V. Balzani, F. Barigelletti, S. Campagna, P. Belser, A. von Zelewsky, Coord. Chem. Rev. 84 (1988) 85.

[3] (a) H. Le Bozec, T. Renouard, Eur. J. Inorg. Chem. (2000) 229. (b) E.S. Handy, A.J. Pal, M.F. Rubner, J. Am. Chem. Soc. 121 (1999) 3525. (c) T. Klumpp, M. Linsenmann, S.L. Larson, B.R. Limoges, D. Bürssner, E.B. Krissinel, C.M. Elliott, U.E. Steiner, J. Am. Chem. Soc. 121 (1999) 1076.

[4] (a) S.I. Khan, A.E. Beilstein, M.T. Tierney, M. Sykora, M.W. Grinstaff, Inorg. Chem. 38 (1999) 5999. (b) I. Hamachi, S. Tanaka, S. Tsukiji, S. Shinkai, S. Oishi, Inorg. Chem. 37 (1998) 4380. (c) I. Hamachi, S. Tsukiji, S. Shinkai, S. Oishi, J. Am. Chem. Soc. 121 (1999) 5500. (d) H.K. Rau, N. DeJonge, W. Haehnel, Proc. Natl. Acad. Sci. USA 95 (1998) 11 526.

[5] S.I. Khan, A.E. Beilstein, G.D. Smith, M. Sykora, M.W. Grinstaff, Inorg. Chem. 38 (1999) 2411.

[6] D.W. Dixon, N.B. Thornton, V. Steullet, T. Netzel, Inorg. Chem. 38 (1999) 5526.

[7] (a) A. Del Guerzo, A. Kirsch-De Mesmaeker, M. Demeunynck, J. Lhomme, J. Chem. Soc., Dalton Trans. (2000) 1173. (b) D.J. Hurley, J.R. Roppe, Y. Tor, Chem. Commun. (1999) 993. (c) S.A. Tysoe, R. Kopelman, D. Schelzig, Inorg. Chem. 38 (1999) 5196. (d) W. Bannwarth, W. Pfleiderer, F. Müller, Helv. Chim. Acta 74 (1991) 1991. (e) W. Bannwarth, F. Müller, Helv. Chim. Acta 74 (1991) 2000.

[8] (a) I. Hamachi, H. Takashima, Y.-Z. Hu, S. Shinkai, S. Oishi, Chem. Commun. (2000) 1127. (b) S.H. Bossmann, M.F. Ottaviani, D. van Loyen, H. Dürr, C. Turro, Chem. Commun. (1999) 2487.

[9] H.F.M. Nelissen, A.F.J. Schut, F. Venema, M.C. Feiters, R.J.M. Nolte, Chem. Commun. (2000) 577.

[10] C.W. Roger, M.O. Wolf, Chem. Commun. (1999) 2297.

[11] M.E. Padilla-Tosta, J. Manuel Lloris, R. Martinez-Manez, A. Benito, J. Soto, T. Pardo, M.A. Miranda, M.D. Marcos, Eur. J. Inorg. Chem. (2000) 741.

[12] (a) V.W.W. Yam, A.S.F. Kai, Inorg. Chim. Acta, 300–302 (2000) 82. (b) S.C. Rawle, P. Moore, N.W. Alcock, J. Chem. Soc., Chem. Commun. (1992) 684.

[13] M. Montalti, S. Wadhwa, W.Y. Kim, R.A. Kipp, R.H. Schmehl, Inorg. Chem. 39 (2000) 76.

[14] (a) K.O. Johannson, J.A. Lotoski, C.C. Tong, G.S. Hanan, Chem. Commun. (2000) 819. (b) L.A. Worl, W.E. Jones Jr, G.F. Strouse, J.N. Younathan, E. Danielson, K.A. Maxwell, M. Sykora, T.J. Meyer, Inorg. Chem. 38 (1999) 2705. (c) A. Wu, D. Yoo, J.-K. Lee, M.F. Rubner, J. Am. Chem. Soc. 121 (1999) 4883. (d) J.-K. Lee, D. Yoo, M.F. Rubner, Chem. Mater. 9 (1997) 1710.

[15] P. Belser, A. von Zelewsky, M. Frank, C. Seel, F. Vögtle, L. De Cola, F. Barigelletti, V. Balzani, J. Am. Chem. Soc. 115 (1993) 4076.

[16] (a) J. Chen, F.M. MacDonnell, Chem. Commun. (1999) 2529. (b) A.A. Bhuiyan, J.R. Kincaid, Inorg. Chem. 38 (1999) 4759. (c) A.K. Bilakhiya, B. Tyagi, P. Paul, Polyhedron 19 (2000) 1233.

[17] S. Arounaguiri, B.G. Maiya, Inorg. Chem. 38 (1999) 842.

[18] (a) E. Eskelinen, S. Luukkanen, M. Haukka, M. Ahlgren, T.A. Pakkanen, J. Chem. Soc., Dalton Trans. (2000) 2745. (b) Y. Shen, K.A. Walters, K. Abboud, K.S. Schanze, Inorg. Chim. Acta 300–302 (2000) 414. (c) H. Takashima, S. Shinkai, I. Hamachi, Chem. Commun. (1999) 2345. (d) K. Ohkubo, T. Hamada, H. Ishida, M. Fukushima, M. Watanabe, H. Kobayashi, J. Chem. Soc., Dalton Trans. (1994) 239. (e) J.E. Collins, J.J.S. Lamba, J.C. Love, J.E. McAlvin, C. Ng, B.P. Peters, X. Wu, C.L. Fraser, Inorg. Chem. 38 (1999) 2020. (f) C.P. Horwitz, Q. Zuo, Inorg. Chem. 31 (1992) 1607. (g) E.H. Yonemoto, R.L. Riley, Y. Il Kim, S.J. Atherton, R.H. Schmehl, T.E. Mallouk, J. Am. Chem. Soc. 114 (1992) 8081.

[19] D. Hesek, Y. Inoue, S.R.L. Everitt, H. Ishida, M. Kunieda, M.G.B. Drew, Inorg. Chem. 39 (2000) 308.

[20] H.-P. Wu, C. Janiak, G. Rheinwald, H. Lang, J. Chem. Soc., Dalton Trans. (1999) 183.

[21] C. Janiak, S. Deblon, H.-P. Wu, M.J. Kolm, P. Klüfers, H. Piotrowski, P. Mayer, Eur. J. Inorg. Chem. (1999) 1507.

[22] C. Janiak, S. Deblon, H.-P. Wu, Synth. Commun. 29 (1999) 3341.

[23] (a) F. Ebmeyer, F. Vögtle, Chem. Ber. 122 (1989) 1725. (b) W.H.F. Sasse, C.P. Whittle, J. Chem. Soc. (1961) 1347. (c) M. Badger, W.H.F. Sasse, J. Chem. Soc. (1956) 616.

[24] A. Lay, M. Sargeson, H. Taube, Inorg. Synth. 24 (1985) 291.

[25] G. Sprintschnik, H.W. Sprintschnik, P.P. Kirsch, D.G. Whitten, J. Am. Chem. Soc. 99 (1977) 4947.

[26] J.A. Broomhead, C.G. Young, Inorg. Synth. 21 (1982) 127.

[27] (a) E.T. Bell-Loncella, C.A. Bessel, Inorg. Chim. Acta 303 (2000) 199. (b) S. Chakraborty, M.G. Walawalkar, G.K. Lahiri, J. Chem. Soc., Dalton Trans. (2000) 2875. (c) D. Hesek, Y. Inoue, S.R.L. Everitt, H. Ishida, M. Kunieda, M.G.B. Drew, J. Chem. Soc., Dalton Trans. (1999) 3701. (d) J.M. Kelly, C. Long, C.M. O'Connell, J.G. Vos, A.H.A. Tinnemans, Inorg. Chem. 22 (1983) 2818. (e) B.P. Sullivan, D.J. Salmon, T.J. Meyer, Inorg. Chem. 17 (1978) 3334.;

[28] F. Barigelletti, A. Juris, V. Balzani, P. Belser, A. von Zelewsky, Inorg. Chem. 22 (1983) 3335.

[29] (a) M.J. Cook, A.P. Lewis, G.S.G. McAuliffe, V. Skarda, A.J. Thomson, J.L. Glasper, D.J. Robbins, J. Chem. Soc., Perkin Trans. II (1984) 1293. (b) M.J. Cook, A.J. Thomson, Chem. Br. (1984) 914.

[30] A. Juris, S. Campagna, V. Balzani, G. Gremaud, A. von Zelewsky, Inorg. Chem. 27 (1988) 3652.

[31] T. Saji, S.J Aoyagui, Electroanal. Chem. 58 (1975) 401.

[32] V. Skarda, M.J. Cook, A.P. Lewis, G.S.G. McAuliffe, A.J. Thomson, J. Chem. Soc., Perkin Trans. II (1984) 1309.
[33] C.M. Elliott, E.J. Hershenhart, J. Am. Chem. Soc. 104 (1982) 7519.
[34] Y. Ohsawa, M.K. DeArmond, K.W. Hanck, D.E. Morris, J. Am. Chem. Soc. 105 (1983) 6522.
[35] T. Koopmans, Physica 104 (1934) 1.
[36] F. Barigelletti, A. Juris, V. Balzani, P. Belser, A. von Zelewsky, Inorg. Chem. 26 (1987) 4115.
[37] C. Janiak, J. Chem. Soc., Dalton Trans. (2000) 3885.
[38] G.R. Desiraju, T. Steiner, The Weak Hydrogen Bond. In: IUCr Monograph on Crystallography, vol. 9, Oxford Science, Oxford, 1999.
[39] G. Cascarano, A. Altomare, C. Giacovazzo, A. Guagliardi, A.G.G. Moliterni, D. Siliqi, M.C. Burla, G. Polidori, M. Camalli, Acta Crystallogr., Sect. A 52 (1996) C79.
[40] (a) G.M. Sheldrick, SHELXL-97, Program for Crystal Structure Refinement, Göttingen, 1997. (b) SHELXS-97, Program for Crystal Structure Solution, Göttingen, 1997.
[41] (a) M.N. Burnett, C.K. Johnson, ORTEP-III: Oak Ridge Thermal Ellipsoid Plot Program for Crystal Structure Illustrations, Oak Ridge National Laboratory Report ORNL-6895, 1996. (b) L.J. Farrugia, ORTEP3 for Windows, version 1.0.1β, University of Glasgow, Scotland, 1997.
[42] P.J. Steel, F. Lahouse, D. Lerner, C. Marzin, Inorg. Chem. 22 (1983) 1488.